

1 **Acoustic evidence for seasonal resource-tracking migration** 2 **by a top predator of the deep sea**

3
4 William K. Oestreich^{a,*}, Kelly J. Benoit-Bird^a, Briana Abrahms^b, Tetyana Margolina^c, John E.
5 Joseph^c, Yanwu Zhang^a, Carlos A. Rueda^a, John P. Ryan^a

6
7 ^a Monterey Bay Aquarium Research Institute, Moss Landing, CA 95039, USA

8 ^b Center for Ecosystem Sentinels, Department of Biology, University of Washington, Seattle, WA
9 98195, USA

10 ^c Naval Postgraduate School, Monterey, CA 93943, USA

11 *Corresponding author: William K. Oestreich

12 **Email:** woestreich.research@gmail.com

13
14 **Keywords:** deep sea, movement ecology, bioacoustics, migration, resource tracking,
15 phenology, sperm whale (*Physeter macrocephalus*)

16 17 **Abstract**

18 The strategies that animals employ to track resources through space and time
19 are central to their ecology and reflect underlying ecosystem phenology. Deep-sea
20 ecosystems represent Earth's largest habitable space, yet ecosystem phenology and
21 effective animal movement strategies in these systems are unknown. Analyzing seven-
22 plus years of continuous population-level acoustic observations, we find evidence for
23 seasonal, latitudinal migratory movements by sperm whales in the Northeast Pacific.
24 Assessment of size-correlated echolocation click characteristics indicates that all
25 demographic groups undertake seasonal movements in this region. Integration of these
26 population-level empirical results with individual-level movement simulations provides
27 the first evidence of seasonal resource-tracking migration in a deep-sea top predator.
28 While often described as nomadic, we instead find that sperm whales track
29 oceanographic seasonality in a manner similar to many surface ocean predators.
30 Together, these findings elucidate the drivers of this top predator's long-distance
31 movements and shed light on the shrouded phenology of deep-sea ecosystems.

1 Introduction

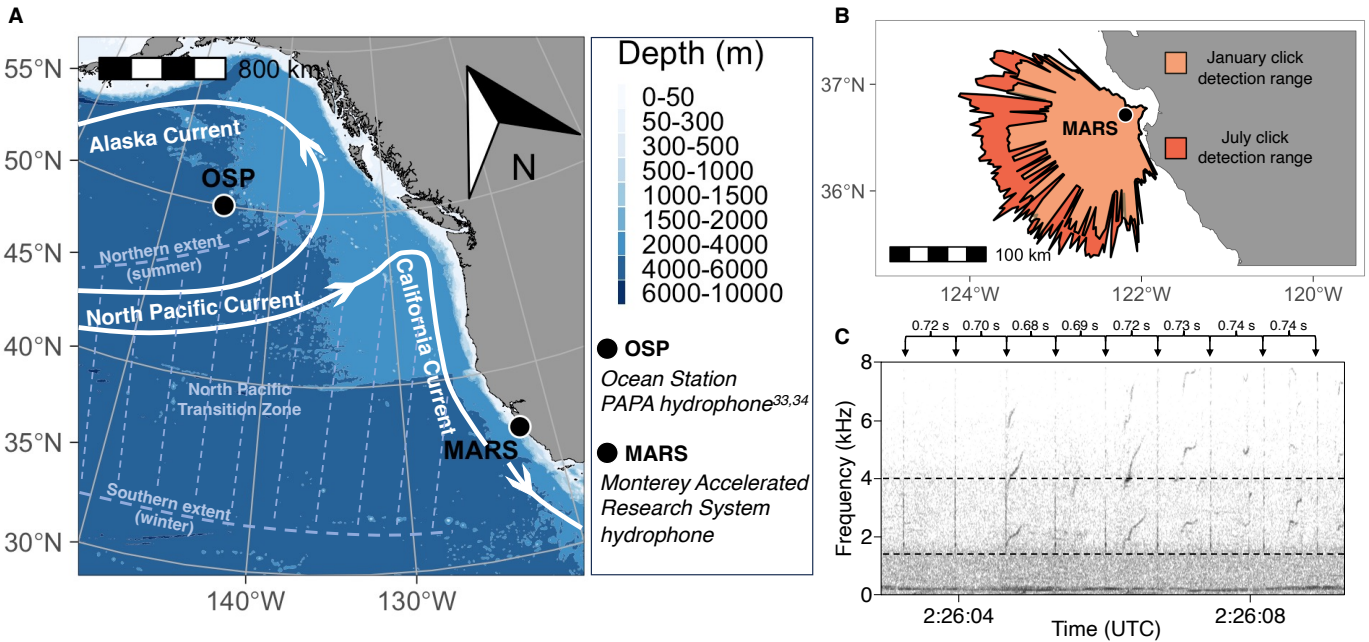
2

3 The movement strategies that animals use to track resources in space and time
4 drive many aspects of their ecology, mediate their ability to respond to environmental
5 perturbations, and provide insight into the spatiotemporal dynamics of the ecosystems
6 they inhabit¹. These individual and group-level movement strategies typically result from
7 spatiotemporal patterns of resource availability², and manifest in distinct patterns of
8 population-level distribution in space and time³. For example, nomadic resource
9 tracking has evolved in aseasonal and unpredictable environments, leading to irregular
10 patterns of individual movement and population distribution⁴. Conversely, in seasonal
11 ecosystems that display spatiotemporal resource dynamics driven by seasonal variation
12 in solar angle, many species have evolved to undertake seasonal migrations⁴.
13 Resource-tracking migrations represent an important connection between ecosystem
14 dynamics and animal movement, closely linking ecosystem phenology with that of
15 seasonal animal migrations^{1,5}. Under this strategy, migrating animals may maximize
16 their resource gain by tracking resource phenology as it propagates across
17 spatiotemporal gradients such as latitudes or elevations⁶. Such resource tracking has
18 been shown to provide a number of individual and population-level benefits, from
19 enabling animals to have more prolonged access to food⁷, to increasing fat gain⁸ and
20 allowing migratory populations to have higher growth rates than sedentary populations⁹.
21 These linkages between resource dynamics and animal movement strategies are
22 increasingly well-understood in seasonal terrestrial^{2,5,8,10}, freshwater¹¹, coastal marine¹²,
23 and epipelagic¹³⁻¹⁸ ecosystems across the globe.

24 Few studies to-date have assessed these connections between ecosystem
25 dynamics and animal movement in Earth's largest habitable space: deep pelagic
26 ecosystems. These oceanic waters deeper than 200m, where little sunlight penetrates,
27 have historically been characterized as stable and aseasonal, but poorly-understood¹⁹.
28 However, a growing body of evidence suggests elements of seasonality in the deep
29 sea. For example, oceanographic studies have documented seasonal variation in the
30 physical and biogeochemical transport of biomass from the surface to the deep²⁰⁻²².

1 Further research has documented seasonality in sightings and biomass of low and mid-
2 trophic level organisms in the mesopelagic^{23–25}. Yet understanding of deep-sea
3 phenology remains limited, particularly for highly-mobile and high-trophic-level animals.
4 This knowledge gap is underpinned by the challenge of making continuous and detailed
5 observations in these ecosystems¹⁹. Given the global extent, high endemic biodiversity,
6 and major role in global biogeochemical cycles of deep pelagic ecosystems,
7 understanding the phenology of these ecosystems and the evolved movement
8 strategies of their inhabitants is important to advance fundamental ecology and inform
9 ecosystem management.

10 We address this gap by integrating long-term passive acoustic monitoring data
11 and movement simulations for a deep pelagic top predator, the sperm whale (*Physeter*
12 *macrocephalus*). Sperm whales are a deep-diving oceanic predator, diving to depths of
13 hundreds-to-thousands of meters²⁶ to forage on diverse deep pelagic prey²⁷. Thus,
14 studying the movement patterns of these ocean giants can provide a rare window into
15 the phenology of the deep-sea environment. In addition, sperm whales produce the
16 loudest known biological sounds²⁸ which not only reveal the presence of this often-
17 cryptic species over large ocean volumes, but also transmit rich behavioral and
18 demographic information about detected individuals. Echolocation clicks are central to
19 the foraging ecology of sperm whales in the low-light conditions of the deep sea, and
20 further indicate individuals' behavioral state (foraging), size (both inter-click-interval²⁹
21 and inter-pulse-interval within individual clicks³⁰ correlate with size), and sex and age-
22 class (sperm whales are sexually dimorphic, with males being much larger³¹). Sperm
23 whales use echolocation in both the meso- and bathypelagic³² to locate a variety of
24 squid and fish prey species²⁷. As a result, monitoring patterns of sperm whale
25 echolocation click detection can provide insight into the phenology of both this top
26 predator and the deep pelagic ecosystems in which they forage.



1
2 **Figure 1. Study system and methods.** (A) The Northeast Pacific Ocean, showing the location of
3 passive acoustic recordings from the present study (Monterey Accelerated Research System (MARS) in
4 the Central California Current System) and previous studies^{33,34} (Ocean Station PAPA (OSP) in the Gulf of
5 Alaska). Some map elements adapted from¹³ and⁴⁴. (B) The Central California Current System,
6 indicating winter and summer detection ranges for sperm whale echolocation clicks produced at 500m
7 depth (see Materials and Methods and SI for additional depths) based on average January and July
8 oceanographic conditions over the period 2016-2022. The circle indicates MARS (891m depth). (C)
9 Example spectrogram of audio recorded at MARS on November 30, 2022, showing a period when a
10 single foraging sperm whale's echolocation clicks (impulsive, broadband signals) were clearly visible and
11 audible. Dashed horizontal lines indicate the minimum and maximum frequencies of the automated
12 energy detector used to detect sperm whale echolocation clicks. Note the near-constant inter-click-
13 interval used to discern echolocating sperm whales from other impulsive sound sources in this frequency
14 range (see Materials and Methods for details).

15
16 In the Northeast Pacific (Figure 1A), foraging sperm whales have been detected
17 acoustically year-round, specifically in the Gulf of Alaska (GoA)^{33,34}. Individuals of this
18 population have expansive home ranges, exhibiting wide-ranging movements which
19 include travel between the GoA and the Central California Current System (CCCS;
20 Figure 1A) among other lower-latitude habitats³⁵⁻³⁷. Yet the regularity, seasonality, and
21 behavioral context of such movements have historically remained unclear. Previous
22 studies based on individual-level sightings, genetic, and limited telemetry data have
23 hypothesized that latitudinal movements are likely irregular, resulting from aseasonal
24 nomadic movements³⁶ consistent with the canonical view of dampened (or nonexistent)
25 seasonality in the deep sea¹⁹. Yet recent acoustic studies in the GoA have suggested
26 seasonality in foraging sperm whales' presence^{33,34,38}, challenging the hypothesis of

1 aseasonal nomadic movements. Others have suggested that long-distance latitudinal
2 movements represent migration between distinct high-latitude foraging and low-latitude
3 breeding habitats³⁹, akin to the seasonal migrations of many baleen whales. Sex-
4 specific partial seasonal migration (with only adult males undertaking migration to higher
5 latitudes) has also been hypothesized based on individual-level sightings data^{31,40}, but
6 both sexes have been observed in both the GoA³⁶ and CCCS^{37,41}. Further, individuals
7 with small body size (females and juveniles) are heard year-round in the GoA³⁸, refuting
8 the hypothesis that only adult males undertake these long-distance movements to high
9 latitudes. While individual-level telemetry data can often provide sufficient sample sizes
10 to understand population-level seasonal movement strategies¹³, such data is extremely
11 limited for this sperm whale population, with only two published individual tag
12 deployments of sufficient duration to capture seasonal movements^{13,35}. As with most
13 inhabitants of deep pelagic ecosystems, this murky understanding of sperm whales'
14 movement strategies arises from the challenge of observing their population-level
15 behavior persistently at sufficient scale^{42,43} and limited understanding of phenology in
16 their foraging habitat.

17 Here, we investigate the strategies underlying movements of this deep pelagic
18 top predator in the Northeast Pacific. We consider a hypothesis of seasonal resource-
19 tracking migration akin to that observed in many surface ocean and terrestrial
20 predators^{13,16} alongside three previously-hypothesized movement strategies: nomadic
21 resource tracking³⁶, seasonal migration between distinct habitats^{35,39}, and sex-specific
22 partial seasonal migration^{31,40}. We test these hypotheses by first applying automated
23 acoustic detection methods to more than seven years of passive acoustic recordings in
24 order to discern seasonal and interannual patterns of foraging sperm whale presence in
25 the Central California Current System as compared to the Gulf of Alaska. Passive
26 acoustic monitoring approaches provide a valuable Eulerian lens to assess population-
27 level animal distributions and behavior⁴⁵, particularly in largely-inaccessible oceanic
28 ecosystems¹⁷, when Lagrangian tracking data (e.g., telemetry) is scarce (as with sperm
29 whales in the Northeast Pacific), and in cases where information beyond presence
30 alone (e.g., behavioral state) can be discerned from the properties of detected acoustic

1 signals⁴⁶. We then integrate these empirical patterns with simulations of individual-level
2 movement driven by each of the hypothesized movement strategies. Hypothesis-testing
3 using this integrated approach allows us to (i) determine the unknown seasonality and
4 regularity of foraging sperm whale presence in the Central California Current System,
5 (ii) evaluate the individual-level strategies underlying sperm whales' wide-ranging
6 foraging movements in the deep ocean, and (iii) consider the seasonal and interannual
7 flexibility afforded by these movement strategies in the context of rapid environmental
8 change.

9

10 **Results**

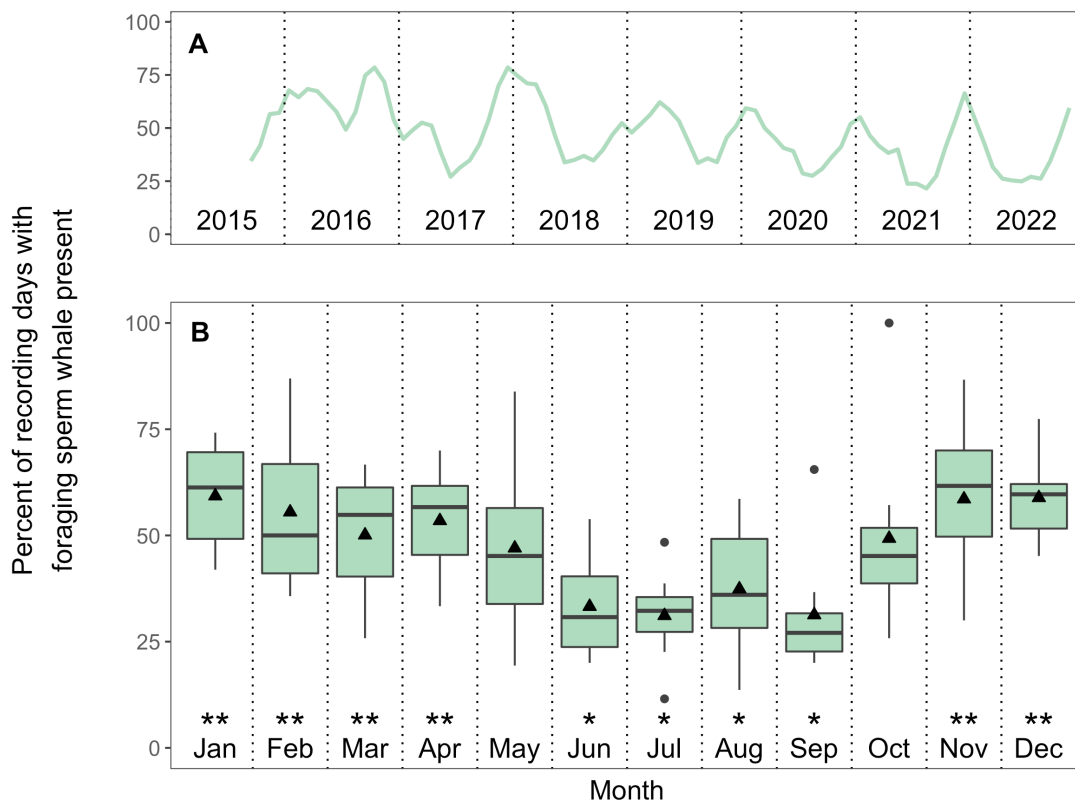
11

12 **Seasonality in acoustic detection**

13 Acoustic detection revealed year-round, seasonally-varying presence of foraging
14 sperm whales in the CCCS (Figure 2). The frequency of foraging sperm whale presence
15 in the average annual cycle reached a maximum in January (mean of 59.3% of days
16 present) and a minimum in July (mean of 31.1% of days present). Monthly percent of
17 days with foraging sperm whale presence is a useful metric in this context for multiple
18 reasons: (1) it provides sufficient temporal resolution to assess seasonal trends, the
19 primary timescale of focus in this study; (2) automated detector performance is very
20 high at daily resolution (Figure S1), providing high confidence in this metric; and (3) this
21 metric matches that used in previous studies of foraging sperm whale presence
22 elsewhere in the Northeast Pacific^{33,34}, allowing for direct comparison of seasonal
23 presence of foraging whales across latitudes. June – September had a significantly
24 lower mean percent of days with presence as compared to the January maximum, and
25 November – April had a significantly higher mean percent of days with presence as
26 compared to the July minimum (Figure 2B). A generalized additive model (GAM)
27 revealed a significant relationship between monthly percent of days with presence and
28 month, with year nested as a random effect ($p < 0.001$; 45.4% deviance explained;
29 Figure S2), further indicating seasonality in foraging sperm whale presence in the
30 CCCS. Detection seasonality did not result from seasonal changes in ambient noise or

1 maximum detection range. Maximum click detection range was slightly greater during
 2 the summer minimum in click detections relative to detection range during the winter
 3 detection maximum (Figures 1B, S3), suggesting that the degree of seasonality shown
 4 here (Figure 2B) is a conservative estimate. Interannually, the percent of recording days
 5 on which foraging sperm whales were detected varied little, with the exception of 2016
 6 (Figure 2A). Foraging sperm whales were detected on 63.4% of recording days in 2016,
 7 whereas the percentage in all other years varied between 38.6-49.9%.

8



9

10 **Figure 2. Variability in foraging sperm whale presence.** (A) Monthly percent presence over the full
 11 study period (smoothed with a 3-month running mean). (B) Annual cycle of echolocating sperm whale
 12 presence over the full study period (Aug 2015 – Dec 2022). Boxplots show the median (center line), mean
 13 (triangle), 25th-75th percentile (box), $\pm 1.5 \times IQR$ (whiskers), and outlying points. *Indicates statistically-
 14 significant difference in mean relative to the maximum month (January). **Indicates statistically-significant
 15 difference in mean relative to the minimum month (July). See Figure S2 for additional statistical
 16 assessment of seasonality.

17

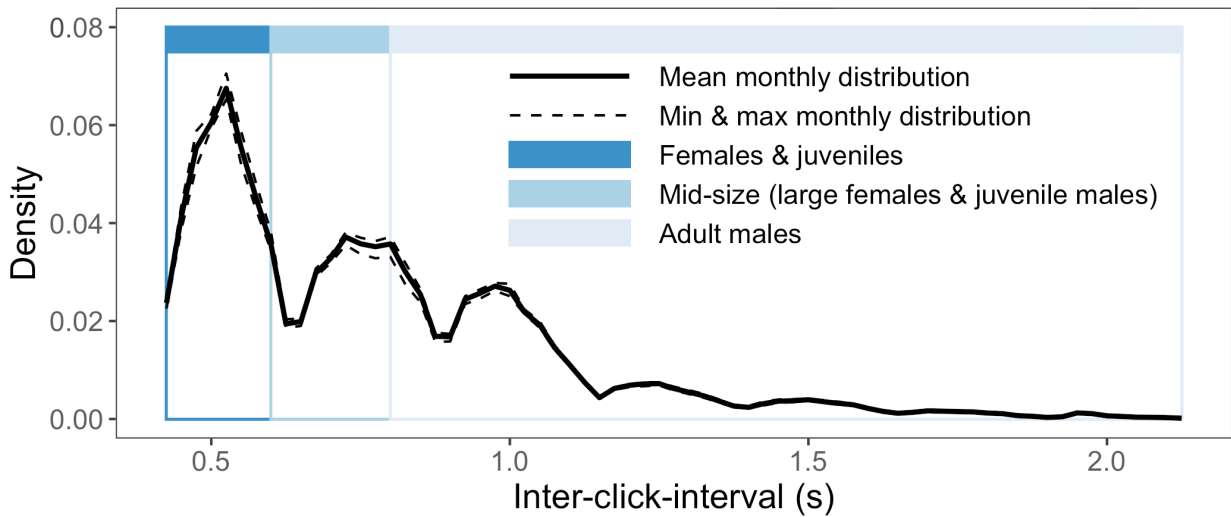
18

19

1 **Seasonality of acoustically-detected demographic groups**

2 Inter-click-interval (ICI) can be used as a proxy for body-size and therefore
3 demographic groups of acoustically-detected individuals in this sexually-dimorphic
4 population²⁹. Similar to acoustic results from the GoA³⁸, we detect three clear modes of
5 ICI (Figure 3). We found no seasonality or interannual variation in the distribution of
6 detected ICIs (and therefore, demographic groups): ANOVA on natural log-transformed
7 ICI data indicated no significant relationship between month ($F = 1.52, p > 0.14$) or year
8 ($F = 1.70, p > 0.12$) and ICI. Further, we detected individuals with both large body size
9 (adult males, $ICI > 0.8$ s^{29,38}) and small body size (females and juveniles, $ICI < 0.6$ s^{29,38})
10 in every individual month of the seven-plus year study period.

11



12

13 **Figure 3. Inter-click-interval (ICI) monthly distributions.** Solid line represents the mean monthly
14 distribution of ICI for detected sperm whale echolocation clicks over the full study period. Dashed lines
15 represent the minimum and maximum monthly ICI distributions at each ICI value. ANOVA on natural log-
16 transformed ICI data showed no significant effect of month ($F = 1.52, p > 0.14$) or year ($F = 1.70, p >$
17 0.12) on ICI. Colors indicate the demographic groups associated with ICI values as per references^{29,38}.

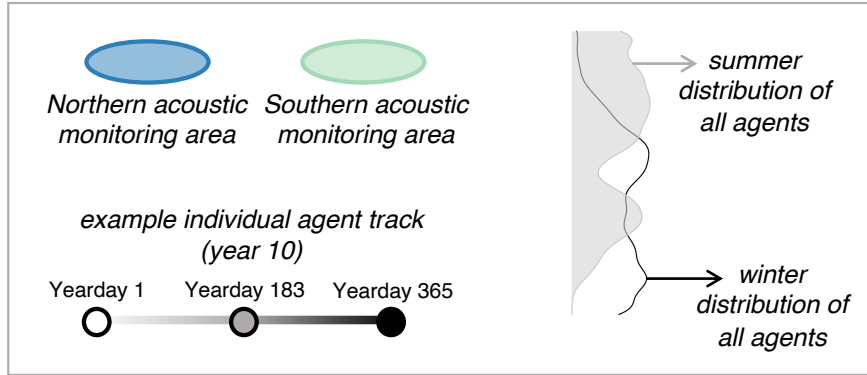
18

19

20 **Comparison of individual-level movement simulations and population-level**
21 **empirical observations**

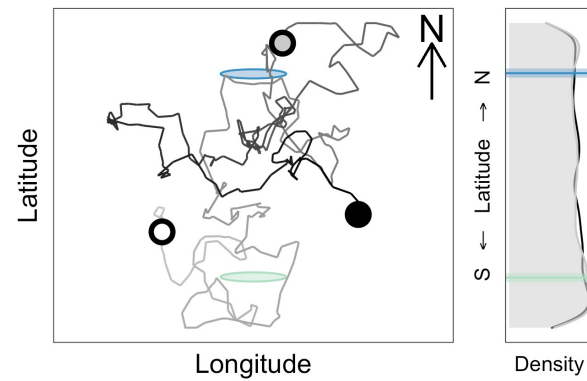
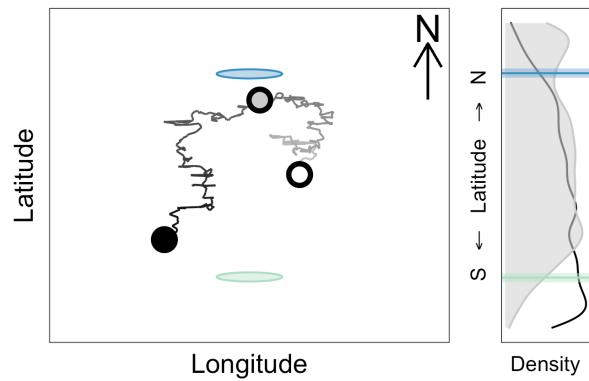
22 Simulations of individual-level movement (Figure 4) yielded qualitatively and
23 quantitatively-distinct patterns in the seasonal-latitudinal distribution (Figure 4) and
24 seasonal acoustic detection (Figure 5) of agents, dependent on the movement strategy

1 employed. The simulation of seasonal resource tracking agents yielded year-round
2 presence with moderate seasonality at both southern and northern listening ranges
3 (Figure 4A), peaking in the winter and summer for the southern and northern listening
4 ranges, respectively (Figure 5B). The seasonal patterns of acoustic detection arising
5 from seasonal resource-tracking migration represented the only simulated results
6 matching the defining qualities of empirically-observed patterns: year-round presence
7 with substantial and opposite seasonality at both higher and lower-latitude listening
8 ranges (Figure 5). Agents following nomadic resource tracking decision rules showed
9 no seasonality in detection at northern or southern listening ranges (Figure 5B), driven
10 by similar winter and summer latitudinal distributions (Figure 4B). Agents undertaking
11 seasonal migrations between distinct habitats showed strong and opposite seasonality
12 in latitudinal distribution (Figure 4C). This simulation yielded high levels of detection
13 during winter and zero detections during summer at the southern listening range, while
14 the northern listening range showed high levels of detection during summer and zero
15 detections during winter (Figure 5B). Simulation of sex-specific partial seasonal
16 migration resulted in strong seasonality in detection at the northern listening range (high
17 levels of detection in summer, zero detections in winter) and year-round detection with
18 weak seasonality at the southern listening range (Figure 4D; Figure 5B). Simulated
19 acoustic detection patterns for seasonal resource-tracking migration were also
20 quantitatively most similar to empirical acoustic detection, yielding a root-mean-square
21 deviation among monthly means of only 15.6% (Figure 5B). All other simulated
22 movement strategies resulted in greater deviance from empirical observations in
23 monthly acoustic detections (22.4% for nomadic resource tracking, 31.7% for seasonal
24 migration between distinct habitats, 31.9% for sex-specific partial seasonal migration;
25 Figure 5B).



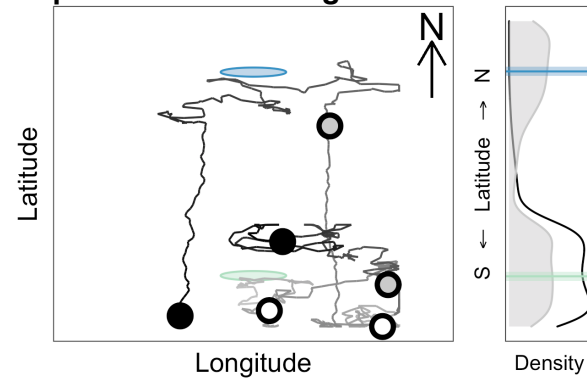
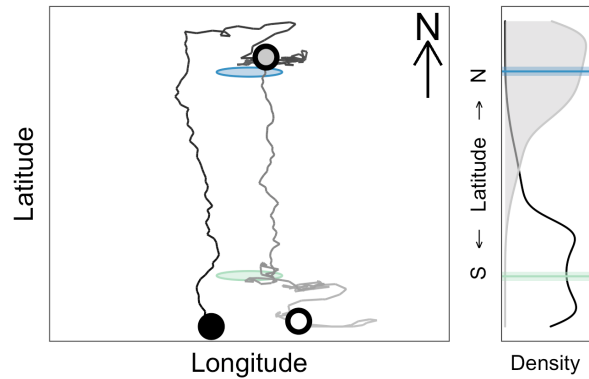
A: Seasonal resource-tracking migration

B: Nomadic resource tracking



C: Seasonal migration between distinct habitats

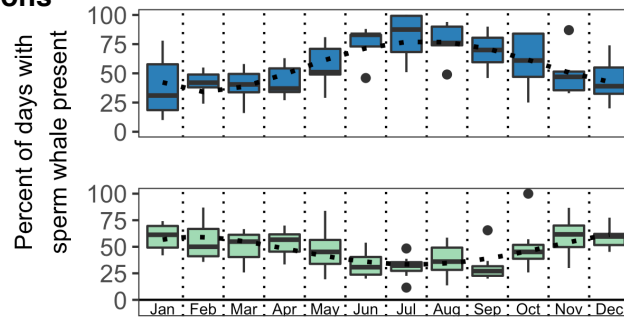
D: Sex-specific partial seasonal migration



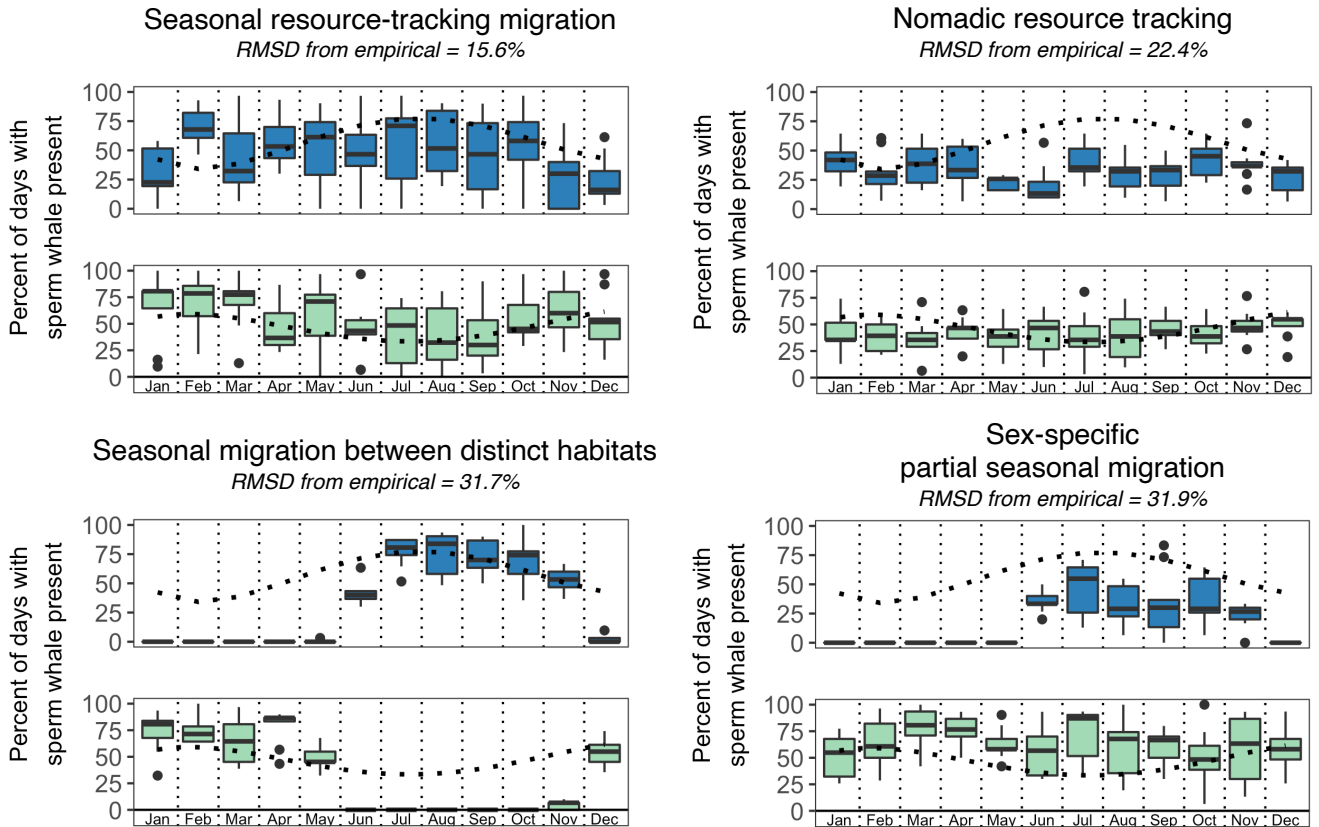
1
2
3
4
5
6
7
8
9
10

Figure 4. Simulated individual-level movement strategies. Top panel provides a legend for simulation results. In each of the bottom panels A-D, one individual agent's track (two agents, one female and one male, in the case of sex-specific partial seasonal migration) is shown from year 10 of the simulation alongside the summer and winter distribution of all agents over years 2-10. Circular acoustic monitoring areas appear elliptical due to distortion of the simulation domain in this visualization to highlight individual agent tracks. **(A)** Seasonal resource-tracking migration. **(B)** Nomadic resource tracking. **(C)** Seasonal migration between distinct habitats. **(D)** Sex-specific partial seasonal migration, showing one migratory (male) and one resident (female) individual track.

A: Empirical observations



B: Simulations



1

2 **Figure 5. Comparison of empirical and simulated acoustic detection seasonality under different**
 3 **hypothesized individual-level movement strategies. (A)** Empirical acoustic detections from the Central
 4 California Current System (green; present study) and the Gulf of Alaska (blue; ^{33,34}). Dotted curves
 5 represent a fourth-order polynomial fit to monthly data from each recording site. **(B)** Acoustic detection at
 6 northern (blue) and southern (green) listening ranges for simulated agents following each of the
 7 hypothesized movement strategies. Boxplots show the median (center line), 25th-75th percentile (box), \pm
 8 $1.5 \times IQR$ (whiskers), and outlying points of monthly acoustic detection over years 2-10 of each simulation.
 9 RMSD refers to the root-mean-square deviation of each simulation's monthly mean acoustic detection
 10 results across both hydrophones relative to empirical observations. Empirical data fourth-order polynomial
 11 from (A) is overlaid on all simulated results.

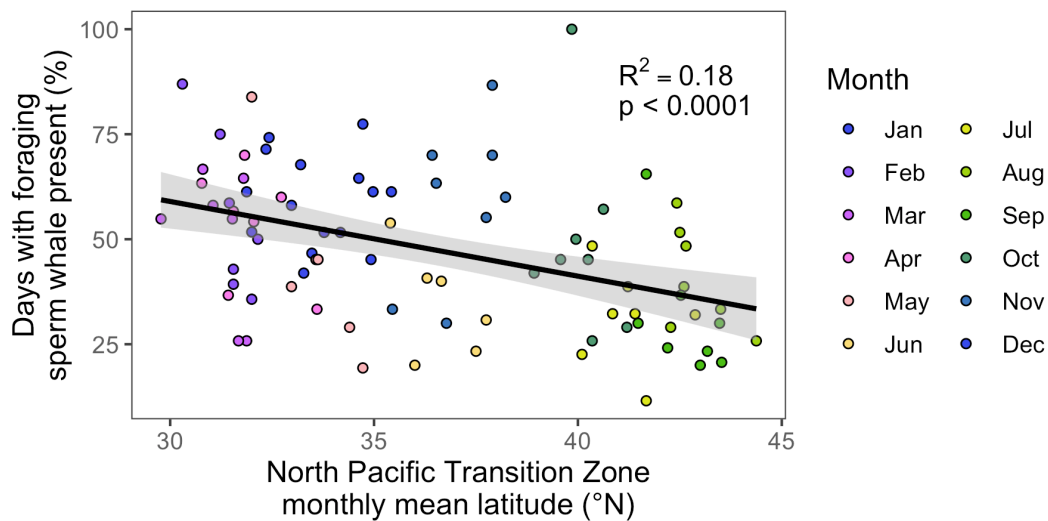
12

13

1 **Seasonality of movement in relation to seasonally-shifting oceanographic habitat**

2 Monthly percent presence of foraging sperm whales also correlated with
3 oceanographic seasonality in the North Pacific Ocean (Figure 6). The latitude of the
4 North Pacific Transition Zone (NPTZ), which has previously been correlated with the
5 seasonal-latitudinal movements of diverse surface ocean predators, was inversely
6 correlated with foraging sperm whale presence in the CCCS. Monthly sperm whale
7 detection rates were highest in winter when the NPTZ is at its lowest latitudinal extent,
8 and sperm whale detection rates were lowest in summer when the NPTZ is at its
9 highest latitudinal extent (Figure 6, Figure 1A).

10



11

12 **Figure 6. Foraging sperm whale presence tracks oceanographic seasonality in the Northeast**
13 **Pacific.** Monthly acoustic detection of foraging sperm whales at MARS relative to the monthly mean
14 latitude of the North Pacific Transition Zone (NPTZ; see Methods and Figure S5 for details).

15

16

17 **Discussion**

18

19 Animals' movement strategies shape their ecology and their ability to respond to
20 environmental perturbations. Moreover, these strategies offer a window into revealing
21 the spatiotemporal dynamics of the ecosystems they inhabit¹. Our findings provide the
22 first evidence for seasonal resource-tracking movements by a top predator in the deep

1 ocean, the sperm whale, suggesting seasonal-latitudinal phenological patterns in the
2 meso- and bathypelagic prey on which sperm whales forage. Below, we discuss several
3 lines of evidence supporting this conclusion of seasonal resource-tracking migration in
4 sperm whales. We then consider how these findings advance understanding of this
5 endangered species' foraging and movement behaviors in response to environmental
6 perturbations. More broadly, we discuss how these results advance knowledge of
7 phenology in the poorly-understood deep ocean ecosystems in which sperm whales
8 forage.

9 The long-term acoustic detection results presented here indicate clear
10 seasonality in the latitudinal movements of foraging sperm whales, with greater
11 frequency of echolocation click detection in California during winter (Figure 2B; Figure
12 S2), opposite the known summer peak of detection in the Gulf of Alaska^{33,34} (Figure 5A).
13 Despite this opposite seasonality, foraging sperm whales are detected year-round in
14 both locations. We posit that these patterns indicate a seasonal resource-tracking
15 migration in this population, based on several lines of evidence. First, seasonal
16 resource-tracking migration is the only hypothesized movement strategy allowing for
17 both year-round presence and significant seasonality in presence across latitudes
18 (Figure 4A; Figure 5B), matching empirical observations (Figure 5A). Nomadism yields
19 relatively uniform latitudinal distributions and year-round but non-seasonal acoustic
20 detection (Figure 4B; Figure 5B). Seasonal migration between distinct habitats (Figure
21 4C; Figure 5B) leads to seasonality in acoustic detection, but does not allow for year-
22 round detection across latitudes. Sex-specific partial seasonal migration similarly does
23 not allow for year-round detection across latitudes, and only results in significant
24 seasonality at some latitudes (Figure 4D; Figure 5B). Additionally, if sex-specific partial
25 seasonal migration were occurring, we would expect the migratory demographic
26 (previously hypothesized to be adult males^{31,40}, with larger body sizes and higher inter-
27 click-intervals (ICI)) to drive seasonal patterns in the distribution of detected ICIs. Yet
28 we do not observe any significant seasonal shifts in the monthly distribution of detected
29 ICIs in California, detecting clicks consistent with female, juvenile, and adult male body
30 sizes year-round (Figure 3). We also find no relationship between monthly mean ICI and

1 monthly percent presence (Figure S4), further indicating that the seasonal pattern
2 observed in Figure 2 is not driven by adult males alone. These results are consistent
3 with long-term acoustic results from the GoA which also show year-round use of high
4 latitudes by females and juveniles³⁸. This growing body of evidence from long-term,
5 persistent, population-level observations via passive acoustics is inconsistent with the
6 individual-sightings-based hypothesis of sex-specific latitudinal segregation, likely
7 arising from differences in the scale and persistence of observation^{42,43}.

8 The results presented here for the CCCS and previously for the GoA^{33,34}
9 specifically document the presence of foraging (echolocating) individuals, underscoring
10 that sperm whales are actively foraging in these study locations and are not only
11 present for non-foraging behaviors (e.g., mating). But what resource or resource-rich
12 habitat are these sperm whales tracking seasonally in the Northeast Pacific?
13 Characterizing the widespread, deep-dwelling, and diverse prey of sperm whales across
14 the Northeast Pacific is a daunting observational task—instead we rely on
15 characterizing the seasonally-shifting North Pacific Transition Zone, the dominant
16 foraging habitat which numerous surface ocean predators track in this ocean basin^{13,47}.
17 We tested whether sperm whales' acoustically-inferred seasonal movements similarly
18 track seasonal-latitudinal patterns in the NPTZ. We find support for this hypothesis, with
19 higher detection of foraging sperm whales in California when the NPTZ is at lower
20 latitude and higher detection in the GoA when the NPTZ is at higher latitude (Figure 6).
21 This similar resource tracking behavior by top predator of the deep ocean to that
22 previously documented for surface ocean predators¹³ suggests ecological linkages
23 between surface and deep ocean processes and seasonality (discussed in greater
24 detail below).

25 This discovery of resource-tracking migratory movements by sperm whales has
26 implications for understanding this deep ocean predator's fundamental ecology and
27 ability to adapt to rapid environmental change. Seasonal resource-tracking migrations in
28 terrestrial and epipelagic populations typically evolve as a strategy to maximize
29 resource gain in dynamic, seasonal ecosystems^{1,4,8}. Interannual variability around the
30 average seasonal-latitudinal patterns exhibited by foraging sperm whales (Figure 2)

1 suggests that the cues driving their latitudinal movements are not fixed seasonal cues
2 (e.g., day length), thus affording flexibility to respond to environmental variation and
3 change. More specifically, sperm whales were most often detected in the CCCS during
4 2016 (Figure 2A), a year in which a persistent marine heatwave combined with a strong
5 El Niño to drive widespread biological impacts in both the CCCS⁴⁸ and GoA⁴⁹. By
6 exhibiting a movement strategy driven by resource tracking rather than fidelity to a fixed
7 foraging area or migratory schedule, sperm whales appear to respond flexibly to
8 interannual variability in oceanographic conditions (Figure 2A; ⁴⁴). Such flexibility is
9 often characteristic of greater resilience to environmental perturbations⁵⁰ including
10 marine heatwaves⁵¹. Understanding the individual and population-level outcomes of
11 such flexibility in this sperm whale population remains an important and rich area for
12 future study.

13 While the specific cues that enable this seasonal resource-tracking migration
14 remain unclear, some combination of individual and social information likely influences
15 these movements. As air-breathing predators, sperm whales spend significant time in
16 surface waters subject to seasonal variability in solar irradiation. This provides a direct
17 means of tracking progression of the seasons, perhaps enabling movements influenced
18 by spatiotemporal memory similar to that observed in highly-mobile epipelagic
19 predators¹⁶. Further, sperm whales and other deep-foraging odontocetes are known to
20 plan deep foraging dives from near the surface using long-range echolocation^{26,52}.
21 Given that mesopelagic and bathypelagic prey can display significant heterogeneity in
22 density⁵³, this approach might allow sperm whales to minimize diving effort in areas of
23 low prey density and allot greater time and energy to horizontal movements to track
24 seasonal-latitudinal forage variability. Because sperm whales echolocate to find prey,
25 long-distance acoustic information on the foraging behavior of conspecifics might further
26 direct this search, similar to the “mobile sensory networks” formed by echolocating
27 bats⁵⁴. Social learning of foraging and movement strategies could also play a role^{55,56},
28 as sperm whales are highly-social animals³¹.

29 More broadly, because animal movements evolve to reflect underlying resource
30 dynamics in the ecosystems they inhabit, our findings indicate seasonal-latitudinal

1 variability in elements of the deep pelagic ecosystems in which sperm whales forage.
2 This challenges the view of seasonal stability in the deep ocean, and contributes to a
3 growing body of evidence for seasonal dynamics in these ecosystems. This seasonality
4 likely arises indirectly via interactions between surface and deep waters⁵⁷. For example,
5 diel vertical migration of animals between the meso- and epipelagic can vary seasonally
6 in terms of depth distribution of animals, migration distance, total biomass, and carbon
7 transport^{24,58,59}. In Monterey Bay specifically, total biomass throughout the meso- and
8 epipelagic is at a minimum in spring and summer, rises in the fall, and remains elevated
9 through the winter²⁴, allowing for greater transport of biomass between surface and
10 deep waters during the seasons when foraging sperm whale detections peak in this
11 region (Figure 2B). Many of the sperm whale's primary prey are themselves vertical
12 migrators³², emphasizing the potential link between seasonal processes in the surface
13 ocean and the seasonal-latitude resource tracking in sperm whales documented here.

14 Taken together, our findings not only reveal unexpected seasonal resource-
15 tracking by a top predator in the deep ocean, but also point toward previously
16 underappreciated seasonal variation in light-limited deep pelagic ecosystems. This
17 study underscores the need for additional research to enhance both fundamental and
18 applied ecology on the phenology of deep pelagic ecosystems across trophic levels. A
19 growing suite of technologies, including remotely-operated vehicles, autonomous
20 underwater vehicles, and continuous active and passive acoustic monitoring are
21 providing an unprecedented opportunity to observe and understand deep ocean
22 ecosystems^{19,25,59}. Especially when integrated^{25,60,61}, these tools can continue to shed
23 light on our murky understanding of seasonal processes and animals' resource-tracking
24 strategies in the deep sea. In turn, we can provide more precise scientific insight in
25 support of spatiotemporally dynamic ecosystem management efforts which have to-date
26 been used on land and in the surface ocean⁶², but which may be possible and valuable
27 in open and deep ocean ecosystems⁶³.

28
29
30

1 **Methods**

2

3 **Study site and hydrophone recordings**

4 Acoustic recordings were collected on the continental slope outside Monterey
5 Bay, CA, via icListen hydrophones sequentially deployed on the Monterey Accelerated
6 Research System (MARS) cabled observatory (36° 42.75'N, 122° 11.21'W; depth 891
7 m). These hydrophones recorded at 256 kHz; all recordings were decimated⁶⁴ to a
8 sample rate of 16 kHz before analysis to dramatically reduce the computational time
9 required to run the workflow described below. While directional components of sperm
10 whale echolocation clicks can have a peak frequency exceeding the Nyquist frequency
11 of these 16 kHz audio files²⁸, this sample rate allows for reliable detection of the
12 omnidirectional low-frequency component of these clicks. Previously, these clicks have
13 been reliably detected in audio files with a sample rate as low as 1 kHz³³.

14

15 **Passive acoustic analyses**

16 Sperm whales produce a variety of click types associated with distinct behaviors.
17 The present analysis focused only on “usual” clicks, which are associated with
18 searching for prey³¹ and are hereafter referred to as clicks. We used a two-step
19 automated workflow (detection and filtration) to determine presence or absence of
20 sperm whale clicks at daily resolution.

21 Candidate detections of individual clicks were generated using a band limited
22 energy detection (BLED) approach implemented in Raven Pro v1.6⁶⁵. The BLED
23 “estimates the background noise of a signal and uses this to find sections of signal that
24 exceed a user-specified signal-to-noise ratio threshold in a specific frequency band,
25 during a specific time”⁶⁵. We manually tuned the parameters of a BLED (Table S1) to
26 maximize the chances of detecting sperm whale clicks under a range of background
27 noise scenarios, but this coarse first step in acoustic processing also generated many
28 false positives.

29 These false positives were filtered out in the second step of our automated
30 workflow by searching BLED results for repetitive, evenly-spaced sequences of

1 detections matching the known inter-click interval (ICI) of sperm whale usual clicks (~0.5
2 – 2.0 seconds⁶⁶). Because the intervals between clicks in sperm whale echolocation
3 sequences are largely regular but not exactly constant, we calculated the time
4 difference between each BLED detection (inter-detection interval; IDI), then rounded to
5 the nearest quarter second to enable a search for sequences of detections with a near-
6 constant IDI. Using these rounded IDI values, each day of recording was automatically
7 searched for IDI sequences matching three criteria: (1) rounded IDI must be between
8 0.5 and 2.0 seconds (inclusive); (2) rounded IDI must be constant; and (3) the number
9 of consecutive IDI values meeting criteria (1) and (2) must meet a sufficient number of
10 repetitions (r) to confidently determine sperm whale echolocation click presence. We
11 considered any day with at least one sequence meeting these criteria to have sperm
12 whale clicks present; any day without any sequence meeting these criteria was
13 considered to have such clicks absent. Setting the number of repetitions required (r) to
14 consider clicks present can significantly impact the accuracy of this automated workflow
15 at daily resolution (Figure S1). The optimal value for this parameter was determined via
16 comparison to manual identification of sperm whale search clicks. Manual assessments
17 were completed for one randomly chosen day of each month in both 2016 and 2020, as
18 well as two days of known sperm whale presence near our recording location (Figure 1)
19 in late 2022. These 26 days provided a representative range of soundscape conditions
20 by covering the full seasonal cycle, including periods recorded by each of the two
21 consecutively-deployed hydrophones, and including recording periods both affected
22 (2020) and unaffected (2016) by the change in anthropogenic noise conditions
23 associated with the COVID-19 pandemic⁶⁷. We found optimal performance at $r = 6$,
24 yielding a daily balanced accuracy of 97% (precision = 100%, recall = 94%) and false
25 positive rate of 0% (Figure S1).

26 Using this time series of daily-resolution presence and absence, we then
27 calculated monthly and annual percent of recording days with foraging sperm whales
28 present for each year and month of the time series. This monthly percent presence
29 metric matches the metric used in previous passive acoustic studies on sperm whale
30 echolocation at Ocean Station PAPA in the Gulf of Alaska over the years 1999-2001³³

1 and 2007-2012³⁴. Monthly percent presence values were estimated graphically from
2 these studies and were later used in comparison to simulation results (Figure 5A; see
3 below).

4 Seasonality in the detection of foraging sperm whales in the CCCS was
5 assessed statistically in two ways. First, we used t-tests to identify months with mean
6 detection rates significantly higher or lower than the maximum (January) and minimum
7 (July) monthly means (Figure 2). Second, we constructed a generalized additive model
8 of monthly percent presence as a function of month with year nested as a random effect
9 to test for the deviance in percent presence explained by the seasonal cycle alone
10 (Figure S2). Finally, we calculated the ICI of all detected click sequences in the time
11 series, allowing for statistical assessment of seasonal or interannual effects on ICI
12 distribution (ANOVA, Figure 3) and comparisons of ICI and foraging sperm whale
13 presence (monthly %) (linear regression, Figure S4).

14

15 **Estimation of ambient noise levels, acoustic propagation loss, and detection** 16 **range**

17 To assess seasonality in click detection range at MARS, we evaluated
18 seasonality in both ambient noise levels and acoustic propagation loss between sound
19 source and acoustic receiver. The ambient noise level metric is single-sided mean-
20 square sound pressure spectral density, following ISO 18405 3.1.3.13 (ISO,
21 2017). From daily files of 16 kHz audio data spanning the full study period, daily mean
22 noise levels were computed for the frequency band targeted by the click detector, 1.4 to
23 4 kHz. Daily values were binned by month across years to examine seasonality (Figure
24 S3B).

25 Acoustic propagation loss was modeled for a sound source matching the
26 characteristics of sperm whale echolocation at the frequencies targeted by our
27 automated detection approach. Specifically, we modeled transmission loss for an
28 impulsive sound source at 2.7kHz (the center frequency of the BLED), 185 dB re: 1 μ Pa
29 at 1m (peak level of the omnidirectional low-frequency component of sperm whale
30 echolocation clicks⁶⁸), and source depths of 100, 500 and 1000m (typical of

1 echolocation in foraging sperm whales in many ecosystems^{26,32,67,69}), received at the
2 location of MARS. Propagation loss was modeled for January and July to assess
3 seasonality in click detection range. Oceanographic water column properties for the
4 January and July model runs were calculated as the climatological mean of
5 oceanographic conditions over the period 2016-2022 as estimated by the HYCOM
6 (HYbrid Coordinate Ocean Model) data assimilative system⁷⁰ with 4.8-minute spatial
7 resolution. Acoustic propagation loss was then calculated for each of 360 1° bearings
8 from MARS using a wave-theory parabolic equation model that accounts for absorption
9 in both the water column and the bottom, scattering in the water column and at the
10 surface and bottom, geometric spreading (spherical and cylindrical), refraction, and
11 diffraction⁷¹. Finally, detection range for each source depth and season was estimated
12 for each of these 360 bearings, requiring received level at MARS to exceed 5.0 dB
13 (SNR of the click detector, Table S1) above monthly median ambient noise levels
14 (Figure S3).

15

16 **Simulation of individual-level movement strategies**

17 To test hypotheses regarding the individual-level movement strategies underlying
18 empirically observed patterns of sperm whale foraging, we employed simulations in
19 which agents move through a spatial domain (Figure 4) with two hydrophone “listening
20 ranges” (one at higher latitude and one at lower latitude), analogous to passive acoustic
21 monitoring of sperm whales in the Gulf of Alaska^{33,34} and the Central California Current
22 System (present study). In all simulations, 100 agents moved daily according to
23 strategy-specific decisions over a ten-year period. The spatial domain in which these
24 simulations occur is not meant to specifically represent the spatial dimensions of the
25 North Pacific or hydrophone listening ranges used in the present or previous studies.
26 Instead, this spatial domain provides a simplified arena for testing realistic individual
27 movement strategies⁷² and their influence on population-level spatiotemporal patterns of
28 acoustic detection. Agent step lengths, hydrophone listening ranges, and domain
29 dimensions were scaled proportionally to allow agents to move seasonally without
30 leaving the domain, while also having limited probability of acoustic detection even if

1 present at the latitude of a listening range (i.e., listening ranges cover only a proportion
2 of both the latitudinal and longitudinal dimensions). This approach allows for realistic
3 probabilities of acoustic detection for a large number of individual position-days
4 (365,000 per simulation) without the extreme computational expense of simulating a
5 number of agents comparable to the estimated population size of sperm whales in the
6 eastern North Pacific (~2000⁷³).

7 We used known information about the typical step lengths, turn angles, and
8 seasonality of movement for well-documented movement “syndromes”⁷² to formulate
9 movement decision rules (described below) for agents representing four distinct
10 movement strategies: nomadic resource tracking, seasonal migration between distinct
11 habitats, sex-specific partial seasonal migration, and seasonal resource-tracking
12 migration. We explored the population-level acoustic detection patterns resulting from
13 each of these four movement strategies via four separate simulations with agents
14 subject to these decision rules. At each daily timestep of each ten-year simulation, we
15 recorded each agent’s position and presence or absence in each of the simulated
16 hydrophone listening ranges. The population-level patterns resulting from each
17 simulation were compared to empirical observations of seasonality in sperm whale
18 foraging (Figure 5A) in the Gulf of Alaska^{33,34} and the Central California Current System
19 (present study; Figure 2B). Specifically, we calculated the root-mean-square deviation
20 of simulated monthly mean acoustic detection results from both listening ranges relative
21 to empirical results from the Gulf of Alaska and the Central California Current System.
22 All results in Figure 5B show agent position and acoustic detection statistics for years 2-
23 10 of the simulation to minimize the influence of initial conditions.

24 We simulated nomadic individuals using decision rules previously documented
25 for nomads⁷²: low probability of behavioral state switching between active foraging and
26 searching, small step lengths and uniformly-distributed turn angles during active
27 foraging, and longer step lengths during searching with normally-distributed turn angles
28 (around the initial direction after switching from foraging to searching).

29 We simulated migration between distinct habitats again using the decision rules
30 documented by ⁷²: four months of foraging in a southern range (steps defined by

1 uniform step length and turn angle distributions), two months of northward migration
2 (longer step lengths and normal turn angle distribution centered on north), four months
3 of foraging in a northern range (steps again defined by uniform step length and turn
4 angle distributions), and finally two months of southward migration (longer step lengths
5 and normal turn angle distribution centered on south).

6 We simulated sex-specific partial seasonal migration by assigning 50% of agents
7 to a migratory (male) group and 50% of agents to a resident (female and juvenile)
8 group. Migrants followed the decision rules described above for migration between
9 distinct habitats; residents followed the decisions rules described above for nomadic
10 resource tracking, but only in the southern portion of the simulation domain.

11 We simulated movements to track resources with a shifting seasonal-latitudinal
12 distribution using decision rules similar to those for nomadic resource tracking as
13 described above, but with differences in movement behavior between times and
14 locations of active foraging. Rather than searching in a single direction with turn angles
15 normally-distributed around a randomly-selected initial search direction (as in nomads),
16 agents in this simulation moved between active foraging periods by tracking resources
17 with headings normally-distributed around due north and due south. The probability of
18 northward-centered or southward-centered heading distributions during resource
19 tracking varied seasonally to mimic seasonal shifts in latitudinal forage availability.

20

21 **Comparison to oceanographic seasonality**

22 The North Pacific Transition Zone (NPTZ; Figure 1A) is a major oceanographic
23 feature in the North Pacific Ocean, representing a transition in surface primary
24 productivity between the subpolar and subtropical gyre⁷⁴ and serving as important
25 foraging habitat for a wide range of predators in the surface ocean^{13,47}. The latitudinal
26 position of the NPTZ varies seasonally, reaching its southern extent in the winter and
27 northern extent in the summer (Figure 1A, ⁷⁴). We calculated the monthly latitude of the
28 NPTZ for each month of the MARS acoustic time series as in ⁷⁴, identifying the mean
29 latitude of the 18 °C sea surface temperature (SST) isotherm between 160-180 °W
30 using monthly composite Aqua MODIS 0.025° daytime SST imagery. We then

1 compared the monthly percent of days with foraging sperm whale present to the
2 monthly NPTZ latitude via linear regression.

3

4 **Software**

5 All analyses and visualizations of click detections and individual-level movement
6 strategies were conducted in R version 4.2.0⁷⁵. The map in Figure 1A was created using
7 the R packages “ggOceanMaps”⁷⁶ and “geosphere”⁷⁷. Background noise, acoustic
8 propagation, and satellite-based oceanographic analyses were conducted in Matlab⁷⁸.
9 Candidate click detections were generated using Raven Pro v1.6⁶⁴.

10

11 **Data and code availability**

12 Raw (256 kHz) and decimated (16 kHz) acoustic data from the MARS
13 hydrophone are available here: <https://docs.mbari.org/pacific-sound/>⁷⁹. Code for
14 processing acoustic data, analyzing sperm whale detections, and simulating individual-
15 level movement strategies are available here:
16 https://github.com/woestreich/cachalot_seasonal⁸⁰.

17

18

19 **References**

20

- 21 1. Abrahms, B. *et al.* Emerging Perspectives on Resource Tracking and Animal Movement Ecology.
22 *Trends Ecol. Evol.* **36**, 308–320 (2021).
- 23 2. Mueller, T. *et al.* How landscape dynamics link individual- to population-level movement patterns:
24 a multispecies comparison of ungulate relocation data. *Glob. Ecol. Biogeogr.* **20**, 683–694 (2011).
- 25 3. Mueller, T. & Fagan, W. F. Search and navigation in dynamic environments – from individual
26 behaviors to population distributions. *Oikos* **117**, 654–664 (2008).
- 27 4. Teitelbaum, C. S. & Mueller, T. Beyond Migration: Causes and Consequences of Nomadic
28 Animal Movements. *Trends Ecol. Evol.* **34**, 569–581 (2019).
- 29 5. Aikens, E. O. *et al.* The greenscape shapes surfing of resource waves in a large migratory
30 herbivore. *Ecol. Lett.* **20**, 741–750 (2017).

- 1 6. Armstrong, J. B., Takimoto, G., Schindler, D. E., Hayes, M. M. & Kauffman, M. J. Resource
2 waves: phenological diversity enhances foraging opportunities for mobile consumers. *Ecology* **97**,
3 1099–1112 (2016).
- 4 7. Deacy, W. W. *et al.* Phenological tracking associated with increased salmon consumption by
5 brown bears. *Sci. Rep.* **8**, 11008 (2018).
- 6 8. Middleton, A. D. *et al.* Green-wave surfing increases fat gain in a migratory ungulate. *Oikos* **127**,
7 1060–1068 (2018).
- 8 9. Fryxell, J. M. & Sinclair, A. R. E. Causes and consequences of migration by large herbivores.
9 *Trends Ecol. Evol.* **3**, 237–241 (1988).
- 10 10. Bastille-Rousseau, G. *et al.* Migration triggers in a large herbivore: Galápagos giant tortoises
11 navigating resource gradients on volcanoes. *Ecology* **100**, e02658 (2019).
- 12 11. Brönmark, C. *et al.* There and back again: migration in freshwater fishes. *Can. J. Zool.* **92**, 467–
13 479 (2014).
- 14 12. Lok, E. *et al.* Spatiotemporal associations between Pacific herring spawn and surf scoter spring
15 migration: evaluating a ‘silver wave’ hypothesis. *Mar. Ecol. Prog. Ser.* **457**, 139–150 (2012).
- 16 13. Block, B. A. *et al.* Tracking apex marine predator movements in a dynamic ocean. *Nature* **475**,
17 86–90 (2011).
- 18 14. Boustany, A. M., Matteson, R., Castleton, M., Farwell, C. & Block, B. A. Movements of pacific
19 bluefin tuna (*Thunnus orientalis*) in the Eastern North Pacific revealed with archival tags. *Prog.*
20 *Oceanogr.* **86**, 94–104 (2010).
- 21 15. Oestreich, W. K. *et al.* Acoustic signature reveals blue whales tune life-history transitions to
22 oceanographic conditions. *Funct. Ecol.* **36**, 882–895 (2022).
- 23 16. Abrahms, B. *et al.* Memory and resource tracking drive blue whale migrations. *Proc. Natl. Acad.*
24 *Sci. U.S.A.* **116**, 5582–5587 (2019).
- 25 17. Ryan, J. P. *et al.* Oceanic giants dance to atmospheric rhythms: Ephemeral wind-driven resource
26 tracking by blue whales. *Ecol. Lett.* **25**, 2435–2447 (2022).
- 27 18. Shuert, C. R. *et al.* Decadal migration phenology of a long-lived Arctic icon keeps pace with
28 climate change. *Proc. Natl. Acad. Sci. U.S.A.* **119**, e2121092119 (2022).
- 29 19. Robison, B. H. Deep pelagic biology. *J. Exp. Mar. Biol. Ecol.* **300**, 253–272 (2004).
- 30 20. Dall’Olmo, G., Dingle, J., Polimene, L., Brewin, R. J. W. & Claustre, H. Substantial energy input to
31 the mesopelagic ecosystem from the seasonal mixed-layer pump. *Nat. Geosci.* **9**, 820–823
32 (2016).
- 33 21. Billett, D. S. M., Lampitt, R. S., Rice, A. L., & Mantoura, R. F. C. Seasonal sedimentation of
34 phytoplankton to the deep-sea benthos. *Nature*, **302**, 520-522. (1983)
- 35 22. Lampitt, R. S., Hillier, W. R., & Challenor, P. G. Seasonal and diel variation in the open ocean
36 concentration of marine snow aggregates. *Nature*, **362**, 737-739. (1993).

- 1 23. Girard, F. *et al.* Phenology in the deep sea: seasonal and tidal feeding rhythms in a keystone
2 octocoral. *Proc. R. Soc. B* **289**, 20221033 (2022).
- 3 24. Urmy, S. S., Horne, J. K. & Barbee, D. H. Measuring the vertical distributional variability of pelagic
4 fauna in Monterey Bay. *ICES J. Mar. Sci.* **69**, 184–196 (2012).
- 5 25. Messié, M. *et al.* Coastal upwelling drives ecosystem temporal variability from the surface to the
6 abyssal seafloor. *Proc. Natl. Acad. Sci. U.S.A.* **120**, e2214567120 (2023).
- 7 26. Fais, A. *et al.* Sperm whale echolocation behaviour reveals a directed, prior-based search
8 strategy informed by prey distribution. *Behav. Ecol. Sociobiol.* **69**, 663–674 (2015).
- 9 27. Kawakami, T. A review of sperm whale food. *Sci. Rep. Whales Res. Inst.* **32**, 199–218 (1980).
- 10 28. Møhl, B., Wahlberg, M., Madsen, P. T., Heerfordt, A. & Lund, A. The monopulsed nature of sperm
11 whale clicks. *J. Acoust. Soc. Am.* **114**, 1143–1154 (2003).
- 12 29. Solsona-Berga, A., Posdaljian, N., Hildebrand, J. A. & Baumann-Pickering, S. Echolocation
13 repetition rate as a proxy to monitor population structure and dynamics of sperm whales. *Remote*
14 *Sens. Ecol. Conserv.* **8**, 827–840 (2022).
- 15 30. Gordon, J. C. D. Evaluation of a method for determining the length of sperm whales (*Physeter*
16 *catodon*) from their vocalizations. *J. Zool.* **224**, 301–314 (1991).
- 17 31. Whitehead, H. *Sperm whales: social evolution in the ocean*. (University of Chicago Press, 2003).
- 18 32. Davis, R. *et al.* Diving behavior of sperm whales in relation to behavior of a major prey species,
19 the jumbo squid, in the Gulf of California, Mexico. *Mar. Ecol. Prog. Ser.* **333**, 291–302 (2007).
- 20 33. Mellinger, D. K., Stafford, K. M. & Fox, C. G. Seasonal occurrence of sperm whale (*Physeter*
21 *macrocephalus*) sounds in the Gulf of Alaska, 1999–2001. *Mar. Mammal Sci.* **20**, 48–62 (2004).
- 22 34. Diogou, N. *et al.* Sperm whale (*Physeter macrocephalus*) acoustic ecology at Ocean Station
23 PAPA in the Gulf of Alaska – Part 1: Detectability and seasonality. *Deep Sea Res. 1 Oceanogr.*
24 *Res. Pap.* **150**, 103047 (2019).
- 25 35. Straley, J. *et al.* Depredating sperm whales in the Gulf of Alaska: local habitat use and long
26 distance movements across putative population boundaries. *Endanger. Species Res.* **24**, 125–
27 135 (2014).
- 28 36. Mizroch, S. A. & Rice, D. W. Ocean nomads: Distribution and movements of sperm whales in the
29 North Pacific shown by whaling data and Discovery marks. *Mar. Mammal Sci.* **29**, E136–E165
30 (2013).
- 31 37. Mesnick, S. L. *et al.* Sperm whale population structure in the eastern and central North Pacific
32 inferred by the use of single-nucleotide polymorphisms, microsatellites and mitochondrial DNA.
33 *Mol. Ecol. Resour.* **11**, 278–298 (2011).
- 34 38. Posdaljian, N. *et al.* Sperm Whales Demographics in the Gulf of Alaska and Bering Sea/Aleutian
35 Islands: An Overlooked Female Habitat. *bioRxiv* preprint. (2023).
36 <https://doi.org/10.1101/2023.04.16.537097doi>

- 1 39. Lefort, K. J., Hussey, N. E., Jones, J. M., Johnson, K. F. & Ferguson, S. H. Satellite-tracked
2 sperm whale migrates from the Canadian Arctic to the subtropical western North Atlantic. *Mar.*
3 *Mammal Sci.* **38**, 1242–1248 (2022).
- 4 40. Best, P. B. *Social organization in sperm whales, Physeter macrocephalus*. Springer US, (1979).
- 5 41. Pitman, R. L., Ballance, L. T., Mesnick, S. I. & Chivers, S. J. Killer Whale Predation on Sperm
6 Whales: Observations and Implications. *Mar. Mammal Sci.* **17**, 494–507 (2001).
- 7 42. Jaquet, N. How spatial and temporal scales influence understanding of Sperm Whale distribution:
8 a review. *Mammal Rev.* **26**, 51–65 (1996).
- 9 43. Levin, S. A. The Problem of Pattern and Scale in Ecology: The Robert H. MacArthur Award
10 Lecture. *Ecology* **73**, 1943–1967 (1992).
- 11 44. Diogou, N. *et al.* Sperm whale (*Physeter macrocephalus*) acoustic ecology at Ocean Station
12 PAPA in the Gulf of Alaska – Part 2: Oceanographic drivers of interannual variability. *Deep Sea*
13 *Res. 2 Top. Stud. Oceanogr.* **150**, 103044 (2019).
- 14 45. Oliver, R. Y. *et al.* Eavesdropping on the Arctic: Automated bioacoustics reveal dynamics in
15 songbird breeding phenology. *Sci. Adv.* **4**, eaaq1084 (2018).
- 16 46. Oestreich, W. K. *et al.* Animal-Borne Metrics Enable Acoustic Detection of Blue Whale Migration.
17 *Curr. Biol.* **30**, 4773-4779.e3 (2020).
- 18 47. Polovina, J. J., Howell, E., Kobayashi, D. R., & Seki, M. P. The transition zone chlorophyll front, a
19 dynamic global feature defining migration and forage habitat for marine resources. *Prog.*
20 *Oceanogr.*, **49**, 469-483. (2001).
- 21 48. Morgan, C. A., Beckman, B. R., Weitkamp, L. A. & Fresh, K. L. Recent Ecosystem Disturbance in
22 the Northern California Current. *Fisheries* **44**, 465–474 (2019).
- 23 49. Walsh, J. E. *et al.* The high latitude marine heat wave of 2016 and its impacts on Alaska. *Bull.*
24 *Am. Meteorol. Soc.* **99**, S39–S43.
- 25 50. Merkle, J. A. *et al.* Site fidelity as a maladaptive behavior in the Anthropocene. *Front. Ecol.*
26 *Environ.* **20**, 187–194 (2022).
- 27 51. Cavole, L. M. *et al.* Biological Impacts of the 2013–2015 Warm-Water Anomaly in the Northeast
28 Pacific: Winners, Losers, and the Future. *Oceanography* **29**, 273–285 (2016).
- 29 52. Arranz, P. *et al.* Risso’s dolphins plan foraging dives. *J. Exp. Biol.* **221**, jeb165209 (2018).
- 30 53. Sato, M. & Benoit-Bird, K. J. Spatial variability of deep scattering layers shapes the Bahamian
31 mesopelagic ecosystem. *Mar. Ecol. Prog. Ser.* **580**, 69–82 (2017).
- 32 54. Roeleke, M. *et al.* Insectivorous bats form mobile sensory networks to optimize prey localization:
33 The case of the common noctule bat. *Proc. Natl. Acad. Sci. U.S.A.* **119**, e2203663119 (2022).
- 34 55. Aikens, E. O., Bontekoe, I. D., Blumenstiel, L., Schlicksupp, A. & Flack, A. Viewing animal
35 migration through a social lens. *Trends Ecol. Evol.* **37**, 985–996 (2022).

- 1 56. Oestreich, W. K. *et al.* The influence of social cues on timing of animal migrations. *Nat. Ecol.*
2 *Evol.* **6**, 1617–1625 (2022).
- 3 57. Hernández-León, S. *et al.* Large deep-sea zooplankton biomass mirrors primary production in the
4 global ocean. *Nat. Commun.* **11**, 6048 (2020).
- 5 58. Archibald, K. M., Siegel, D. A. & Doney, S. C. Modeling the Impact of Zooplankton Diel Vertical
6 Migration on the Carbon Export Flux of the Biological Pump. *Glob. Biogeochem. Cycles* **33**, 181–
7 199 (2019).
- 8 59. Fischer, J. & Visbeck, M. Seasonal variation of the daily zooplankton migration in the Greenland
9 Sea. *Deep Sea Res. Part 1 Oceanogr. Res. Pap.* **40**, 1547–1557 (1993).
- 10 60. Benoit-Bird, K. J. & Lawson, G. L. Ecological Insights from Pelagic Habitats Acquired Using
11 Active Acoustic Techniques. *Annu. Rev. Mar. Sci.* **8**, 463–490 (2016).
- 12 61. Urmey, S. S. & Benoit-Bird, K. J. Fear dynamically structures the ocean’s pelagic zone. *Curr. Biol.*
13 **31**, 5086-5092.e3 (2021).
- 14 62. Oestreich, W. K., Chapman, M. S. & Crowder, L. B. A comparative analysis of dynamic
15 management in marine and terrestrial systems. *Front. Ecol. Environ.* **18**, 496–504 (2020).
- 16 63. Maxwell, S. M., Gjerde, K. M., Conners, M. G. & Crowder, L. B. Mobile protected areas for
17 biodiversity on the high seas. *Science* **367**, 252–254 (2020).
- 18 64. Zhang, Y., McGill, P. R. & Ryan, J. P. Optimized design of windowed-sinc anti-aliasing filters for
19 phase-preserving decimation of hydrophone data. *J. Acoust. Soc. Am.* **151**, 2077–2084 (2022).
- 20 65. Charif, R. A., Waack, A. M., & Strickman, L. M. Raven Pro 1.4 user’s manual. (2010).
- 21 66. Wahlberg, M. The acoustic behaviour of diving sperm whales observed with a hydrophone array.
22 *J. Exp. Mar. Biol. Ecol.* **281**, 53–62 (2002).
- 23 67. Ryan, J. P. *et al.* Reduction of Low-Frequency Vessel Noise in Monterey Bay National Marine
24 Sanctuary During the COVID-19 Pandemic. *Front. Mar. Sci.* **8**, (2021).
- 25 68. Zimmer, W. M. X., Tyack, P. L., Johnson, M. P. & Madsen, P. T. Three-dimensional beam pattern
26 of regular sperm whale clicks confirms bent-horn hypothesis. *J. Acoust. Soc. Am.* **117**, 1473–
27 1485 (2005).
- 28 69. Mathias, D. *et al.* Acoustic and diving behavior of sperm whales (*Physeter macrocephalus*) during
29 natural and depredation foraging in the Gulf of Alaska. *J. Acoust. Soc. Am.* **132**, 518–532 (2012).
- 30 70. Chassignet, E. P. *et al.* The HYCOM (hybrid coordinate ocean model) data assimilative system.
31 *J. Mar. Syst.* **65**, 60-83 (2007).
- 32 71. Collins, M. D. A split-step Padé solution for the parabolic equation method. *J. Acoust. Soc. Am.*
33 **93**, 1736–1742 (1993).
- 34 72. Abrahms, B. *et al.* Suite of simple metrics reveals common movement syndromes across
35 vertebrate taxa. *Mov. Ecol.* **5**, 12 (2017).

- 1 73. Moore, J. & Barlow, J. Improved abundance and trend estimates for sperm whales in the eastern
2 North Pacific from Bayesian hierarchical modeling. *Endanger. Species Res.* **25**, 141–150 (2014).
- 3 74. Bograd, S. J., *et al.* On the seasonal and interannual migrations of the transition zone chlorophyll
4 front. *Geophysical Research Letters*, **31**, L17204. (2004).
- 5 75. R Core Team (2022). R: A language and environment for statistical computing. R Foundation for
6 Statistical Computing, Vienna, Austria. <https://www.R-project.org/>.
- 7 76. Vihtakari, M (2022). ggOceanMaps: Plot Data on Oceanographic Maps using ‘ggplot2’. R
8 package version 1.3.4. <https://CRAN.R-project.org/package=ggOceanMaps>.
- 9 77. Hijmans, R (2022). geosphere: Spherical Trigonometry. R package version 1.5-18,
10 <https://CRAN.R-project.org/package=geosphere>.
- 11 78. The MathWorks Inc. (2022). MATLAB version: 9.13.0 (R2022b), Natick, Massachusetts: The
12 MathWorks Inc. <https://www.mathworks.com>.
- 13 79. Ryan, J. *et al.* New Passive Acoustic Monitoring in Monterey Bay National Marine Sanctuary.
14 *OCEANS 2016 MTS/IEEE Monterey*, 1-8 (2016).
- 15 80. Oestreich, W.K. Data and code for: Acoustic evidence for seasonal resource-tracking migration
16 by a top predator of the deep sea. Zenodo. <https://doi.org/10.5281/zenodo.7860426>. Deposited
17 April 24, 2023.
- 18
19

20 **Acknowledgments**

21
22 Thank you to Melissa Chapman and Megan McKenna for discussions which improved this
23 manuscript. This research was supported by the David and Lucile Packard Foundation through the
24 Monterey Bay Aquarium Research Institute. The NSF funded installation and maintenance of the MARS
25 cabled observatory through awards 0739828 and 1114794. W.K.O. was supported by a postdoctoral
26 fellowship from the David and Lucile Packard Foundation through the Monterey Bay Aquarium Research
27 Institute.

28

29 **Author Contributions**

30
31 W.K.O., K.J.B., and J.P.R. conceived the study; W.K.O., K.J.B., and J.P.R. designed the
32 research; J.P.R. collected data; W.K.O., B.A., T.M., Y.Z., C.A.R., and J.P.R. developed methods; W.K.O.,
33 K.B.B, T.M., and J.P.R. performed analyses; and W.K.O. wrote the manuscript with contributions from all
34 authors.

35

1 **Competing Interest Statement**

2

3 The authors declare no competing interests.

Supporting Information for:

Acoustic evidence for seasonal resource-tracking migration

by a top predator of the deep sea

William K. Oestreich^{a,*}, Kelly J. Benoit-Bird^a, Briana Abrahms^b, Tetyana Margolina^c, John E. Joseph^c, Yanwu Zhang^a, Carlos A. Rueda^a, John P. Ryan^a

^a Monterey Bay Aquarium Research Institute, Moss Landing, CA 95039, USA

^b Center for Ecosystem Sentinels, Department of Biology, University of Washington, Seattle, WA 98195, USA

^c Naval Postgraduate School, Monterey, CA 93943, USA

*Corresponding author: William K. Oestreich

Email: woestreich.research@gmail.com

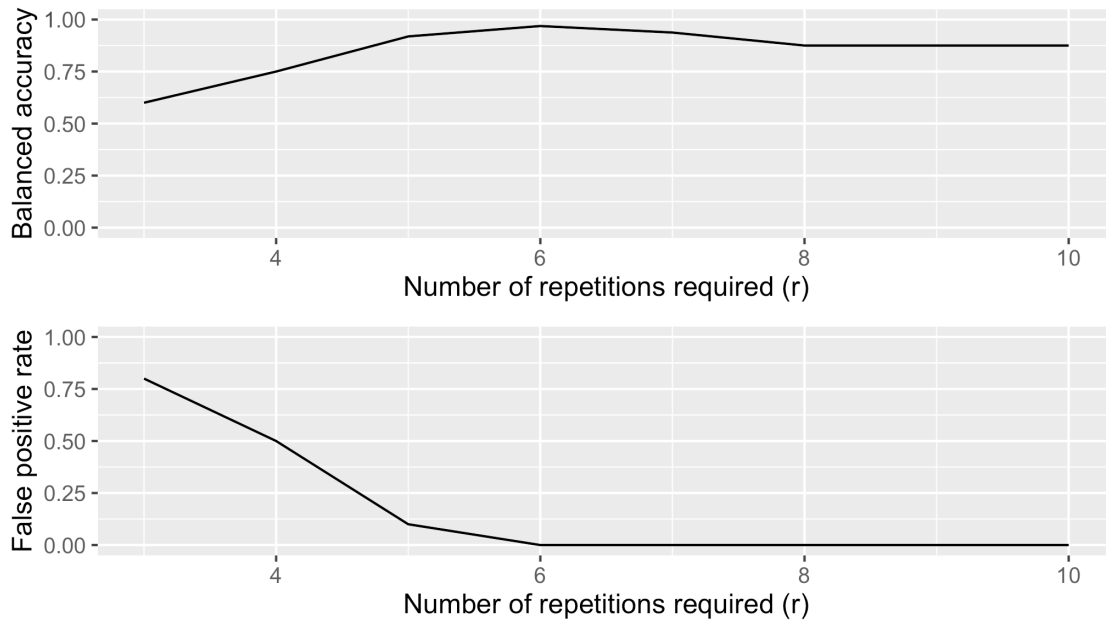


Fig. S1. Performance of automated daily acoustic processing relative to manual assessment. Requiring six repetitions of click detection at near-constant inter-click interval ($r = 6$) yields a daily balanced accuracy of 97% and daily false positive rate of 0%.

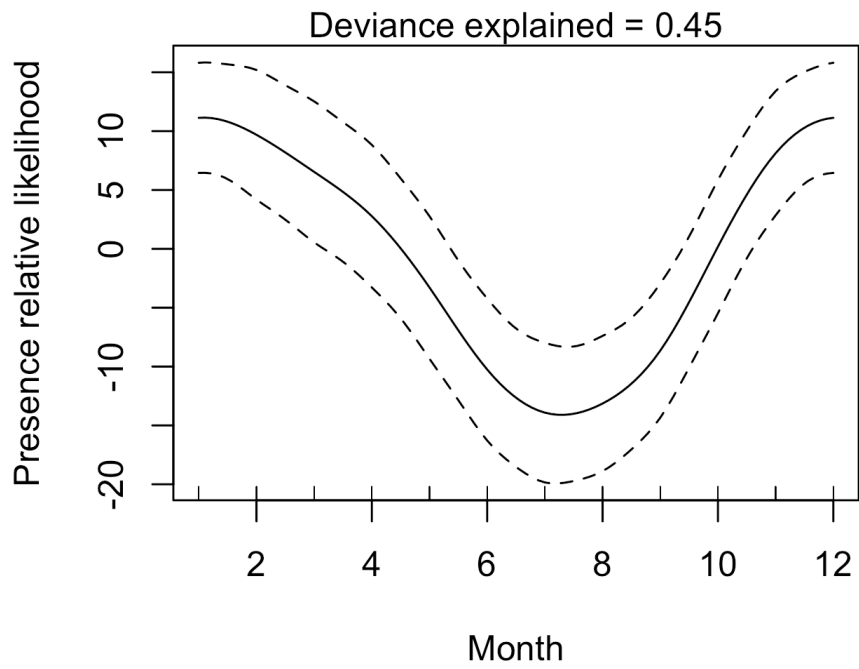


Fig. S2. Generalized additive model fit relationship for monthly foraging sperm whale presence (% of days) and month, with year nested as a random effect.

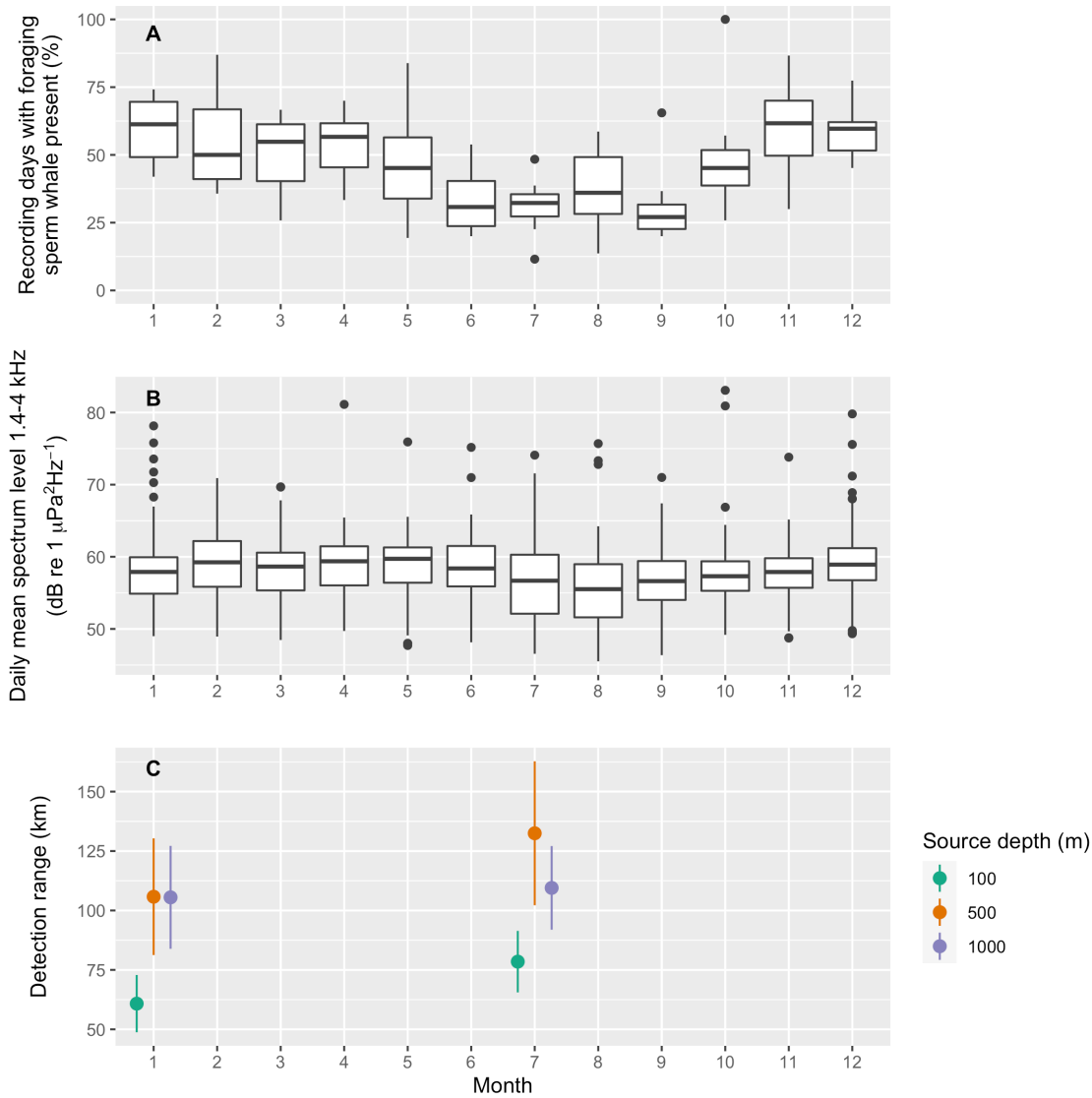


Fig. S3. Seasonal variation in listening conditions at MARS. (A) Average annual cycle of echolocating sperm whale presence averaged over the full study period (Aug 2015 – Dec 2022), reproduced from Figure 2B in the main text. **(B)** Average annual cycle of ambient noise conditions at MARS in the frequency range (1.4-4kHz) targeted by the band limited energy detector employed to identify candidate sperm whale echolocation detections. **(C)** Estimated maximum detection range at MARS for sperm whale echolocation clicks produced at depths of 100, 500, and 1000m during the maximum (January) and minimum (July) months of foraging sperm whale presence. Points and lines represent the mean and standard deviation of 1-degree bearing ranges between 154-311° around MARS, representing the offshore area where 500m and 1000m source depth results are not limited by the shelf break (Figure 1B), and where sperm whales are most likely to be found. See Materials and Methods for information on modeling of acoustic propagation and detection range.

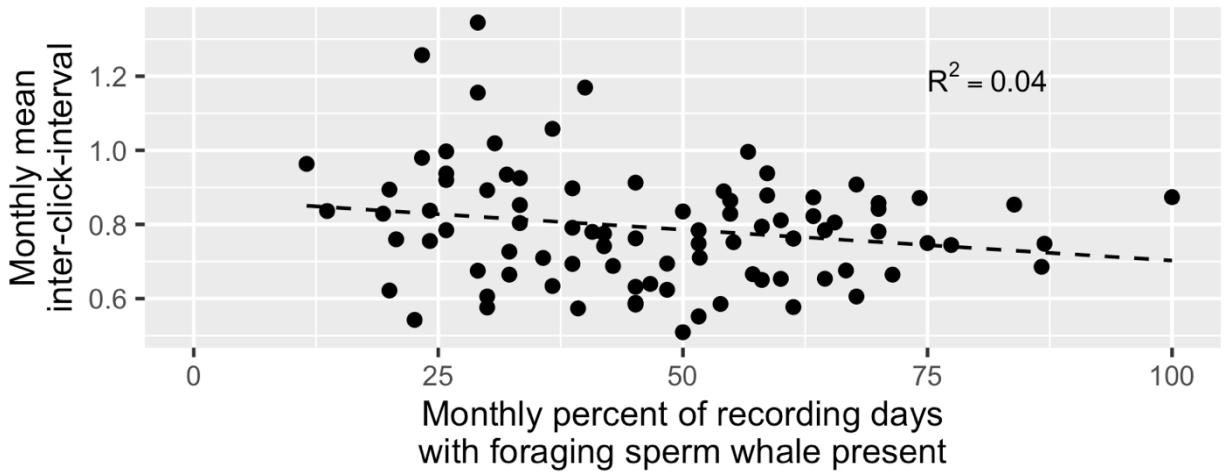


Fig. S4. Additional inter-click-interval (ICI) comparison to monthly foraging sperm whale presence. Monthly mean ICI vs. monthly percent presence, indicating no significant relationship between these variables ($p > 0.05$).

Table S1. Band limited energy detector parameters.

BLED signal calculation	
Min. Frequency	1.4 kHz
Max. Frequency	4.0 kHz
Min. Duration	8.125 ms
Max. Duration	32.5 ms
Min. Separation	32.5 ms
BLED noise calculation	
Block size	2.0 s
Hop size	0.5 s
Percentile	20.0
Signal-to-noise parameters	
Min. Occupancy	70.0%
SNR Threshold	5.0 dB
Spectrogram calculation	
Window	Hann
Window Size	512 samples
Window Overlap	95%